# KKT conditions satisfied using adaptive neighboring in hybrid cellular automata for topology optimization

**Charles L. Penninger[(1)], Andrés Tovar[(2)], Layne T. Watson[(3)], John E. Renaud[(4)]**

[(1,2,4)]University of Notre Dame, Notre Dame, Indiana, USA.
[(3)]Virginia Polytechnic Institute and State University, Blacksburg, Virginia, USA.
[(1)]cpenning@nd.edu, [(2)]atovar@nd.edu, [(3)]ltw@cs.vt.edu, [(4)]jrenaud@nd.edu

## 1. Abstract

The hybrid cellular automaton (HCA) method is a biologically inspired algorithm capable of topology synthesis that was developed to simulate the behavior of the bone functional adaptation process. In this algorithm, the design domain is divided into cells with some communication property among neighbors. Local evolutionary rules, obtained from classical control theory, iteratively establish the value of the design variables in order to minimize the local error between a field variable and a corresponding target value. Karush-Kuhn-Tucker (KKT) optimality conditions have been derived to determine the expression for the field variable and its target. While averaging techniques mimicking intercellular communication have been used to mitigate numerical instabilities such as checkerboard patterns and mesh dependency, some questions have been raised whether KKT conditions are fully satisfied in the final topologies. Furthermore, the averaging procedure might result in cancellation or attenuation of the error between the field variable and its target. Several examples are presented showing that HCA converges to different final designs for different neighborhood configurations or averaging schemes. Although it has been claimed that these final designs are optimal, this might not be true in a precise mathematical sense—the use of the averaging procedure induces a mathematical incorrectness that has to be addressed. In this work, a new adaptive neighboring scheme will be employed that utilizes a weighting function for the influence of a cell's neighbors that decreases to zero over time. When the weighting function reaches zero, the algorithm satisfies the aforementioned optimality criterion. Thus, the HCA algorithm will retain the benefits that result from utilizing neighborhood information, as well as obtain an optimal solution.

**2. Keywords:** Structural optimization, Optimality conditions, Mathematical programming.

## 3. Introduction

Topology optimization strives to distribute material in a design domain in order to maximize a prescribed mechanical performance. Typically, this problem is constrained by the volume or mass of the final structure. To this end, the design domain is divided into a sufficiently large number of elements. In this domain, the optimization algorithm removes or adds material to every element until the process converges. Finite element analysis (FEA) is typically used to evaluate the merit function. Classical gradient-based optimization methods are prohibitively expensive due to the large number of function evaluations. Therefore, new techniques have been proposed in order to efficiently solve topology optimization problems. Rozvany [1] presents a review of two commonly used approaches referred to as Solid Isotropic Microstructure (or Material) with Penalization (SIMP) [2] and Evolutionary Structural Optimization (ESO) [3]. Other approaches include the method of moving asymptotes (MMA) [4] and the homogenization method [5]. A family of methods characterized by its computational efficiency (i.e., naturally parallel algorithms) is the cellular automaton (CA) approach [6, 7, 8, 9, 10], reviewed for topology optimization by Abdalla et al. [11].

In particular, the hybrid cellular automaton (HCA) method [9, 10] is a well developed approach derived from Karush-Kuhn-Tucker (KKT) conditions that combines the CA paradigm (i.e., local optimization rules) with FEA (i.e., global structural analysis) [12]. In this method, local field variables are driven to a desired optimal value by modifying local design variables. Control rules applied to individual elements in the structure are utilized to find the optimal states [10]. This method has been utilized to synthesize noncompliant structures subject to mass, stress, and displacement constraints [13], compliant mechanisms [14], and energy absorbing structures for crashworthiness [15]. The HCA method has been proven to be a globally convergent (under certain assumptions) fixed point iteration scheme [16]. However, the original neighborhood averaging numeric implementation of the HCA method may fail to achieve a KKT point.

The neighboring technique in the HCA method is inspired by the cellular communication occurring in biological structures such as bones [17]. In this way, the algorithm defines an effective field variable value by averaging the values obtained in the vicinity of each element, which results in a reduction of

checkerboard patterns (alternating solid elements and voids resembling a checkerboard) in the final structure. These patterns are undesirable as they are the result of discretization and do not correspond to an optimal continuous distribution of material [18]. In fact, some finite element discretizations make checkerboard patterns appear to be artificially efficient. Some other procedures to deal with checkerboards were reviewed by [18]. These procedures include image processing (e.g., smoothing and filtering), higher-order finite elements, and patches (i.e., superelements on the finite element mesh).

This investigation presents a novel neighboring technique that achieves a KKT point final topology while reducing checkerboarding. This technique is presented using quadrilateral bilinear finite elements. A two-dimesional simply supported beam example is used to show its implementation and its main advantages.

## 4. The hybrid cellular automaton method

In nature, numerous biological structures occur that achieve an efficient form in correspondence with their function. In particular, bone undergoes remodeling precesses to functionally adapt its structure to changes in the local mechanical environment. This process has inspired the development of the hybrid cellular automata (HCA) algorithm as presented by Tovar [17].

This methodology utilizes the cellular automata (CA) computing paradigm where a regular lattice of cells can exist in any finite number of dimensions. Each cell itself represents a discrete dynamical system. The basis for CA is that an overall global behavior can emerge from local rules acting over an automaton that possesses only local state information. In the case of the HCA algorithm, the local state information is determined from a global finite element analysis (FEA). Thus, HCA is a hybrid technique as it utilizes global information to drive local state behavior. The basis of HCA is that complex static and dynamic problems can be simplified to a set of local rules that operate over a lattice of cells that know only their local conditions.

### 4.1. Biologically inspired framework

The CA lattice utilized by the HCA formulation is assumed to model the connected cellular network of osteocytes in bone. Osteocytes are the most abundant cell in bone tissue and are assumed to act as mechonosensors, sensing the mechanical stimulus in a local region. Therefore, if a region of bone is discretized into a regular lattice of cells it is reasonable to assume that each cell will contain one or more osteocytes, surrounded by mineralized tissue. One theory for bone functional adaptation is that bone is remodeled to achieve a local target mechanical stimulus. Thus, this model assumes that local changes in relative density are driven by a mechanical stimulus target differential. Consequently, three variables are required to define the state of each cell $\psi_i(t)$ in the lattice, the relative (or normalized) density $x_i(t)$, the mechanical stimulus $S_i(t)$, and the error signal $e_i(t)$, written

$$\psi_i(t) = \begin{pmatrix} x_i(t) \\ S_i(t) \\ e_i(t) \end{pmatrix}. \tag{1}$$

where $S_i(t) = U_i(t)/x_i(t)$ and $U_i(t)$ is the strain energy in the $i^{th}$ cell.

Osteocytes are also connected with each other through a network of cellular processes, allowing for the passage of various signals. This neighborhood communication is effected in the HCA framework by gathering information from neighboring cells. The effective mechanical stimulus sensed by each cell $\bar{S}_i(t)$ is calculated as the average of the stimuli sensed by all of the cells within the designated neighborhood,

$$\bar{S}_i(t) = \frac{S_i(t) + \sum_{k \in N(i)} S_k(t)}{1 + \hat{N}(i)}, \tag{2}$$

where $S_i(t)$ is the state of mechanical stimulus at location $i$, $S_k(t)$ represents the mechanical stimulus sensed by the $k^{th}$ neighbor, $N(i) = \{\text{indices of neighbors of cell } i\}$, and $\hat{N}(i) = |N(i)|$ is the total number of neighbors in the neighborhood. In the context of CA computing, no restrictions are generally placed on the sized of the neighborhood, only that the neighborhoods are consistent for each cell in the lattice.

As new bone is formed and old bone is removed over time the relative density of each can cell vary, resulting in a change in the modulus of the material. This material behavior is modeled using a power law, which assumes that the material remains locally isotropic. Therefore, the modulus at a location $i$ is calculated as

$$E_i(t) = E_{0i} x_i(t)^p, \tag{3}$$

where $E_{0i}$ is the base modulus for each cell, typically set to the modulus of fully dense bone (assumed to be equivalent to cortical bone), and $p$ is an empirical value, typically satisfying $2 \leq p \leq 3$ [19]. For topology

synthesis problems, the goal is to obtain a structure that has a '0-1' topology, meaning that the structure is comprised of areas of fully dense material ($x_i(t) = 1$) or a void ($x_i(t) = 0$). Ideally the relative density would be a discrete variable (i.e., $x_i(t) \in \{0, 1\}$). For the HCA formulation, the relative density $x_i(t)$ is relaxed such that it is a continuous function (i.e., $0 \leq x_i(t) \leq 1$).

The overall purpose of the bone remodeling process is functional adaptation to variations in bone's mechanical environment to obtain a state of equilibrium. The local rules $\mathbf{R}$ utilized by the HCA framework are designed to model this process. These rules $R_i$ are driven by the mechanical stimulus target differential. Therefore, strength of the remodeling signal is measured by the normalized error between the effective stimulus sensed and the stimulus target,

$$e_i(t) = \frac{\bar{S}_i(t) - S_i^*}{S_i^*}, \tag{4}$$

where $\bar{S}_i(t)$ is the effective mechanical stimulus, which incorporates information from neighboring cells, and $S_i^*$ is the stimulus target. In the context of bone remodeling, a positive error signal would lead to formation, while a negative error signal would lead to resorption. Once the error signal becomes zero, no further remodeling is required and bone returns to equilibrium. The set of local rules $\mathbf{R}$ update the material distribution evolving the structure towards equilibrium according to information gathered from the cells in a prescribed neighborhood.

Previous investigations with HCA have utilized control based rules and a ratio based rule, following the principles of fully stressed design [12]. For the current study, the proportional, integral, and derivative (PID) control strategy will be utilized. The reasoning behind proportional control is that it is assumed that osteoclastic or osteoblastic activity occurs in proportion to the error between a local effective mechanical stimulus and the stimulus target. Various computational models of bone remodeling use some form of proportional control in their remodeling rule [20, 21, 22, 23]. Integral control provides a pathway for including a sense of memory in the adaptation process. Consequently, this can be interpreted as osteocytes storing information from previous states, i.e., $e_i(t-1)$, ..., $e_i(t-T)$. Thus, the remodeling activity is proportional to the cumulative error. The rate of osteoblastic and osteoclastic activity depending on a prediction of the future error signal, based on the current and previous error signals $e_i(t)$ and $e_i(t-1)$, represents a form of derivative control. Hence, the change in relative density $\Delta x_i(t)$ for a cell at location $i$ is given as

$$\Delta x_i(t) = c_p e_i(t) + c_i \int_0^t e_i(\tau)\, d\tau + c_d \Delta e_i(t), \tag{5}$$

where $c_p$, $c_i$, and $c_d$ are the proportional, integral, and derivative control gains, respectively. Therefore, the material update for each cell is

$$x_i(t+1) = \min\left\{\max\left\{0, x_i(t) + c_p e_i(t) + c_i \int_0^t e_i(\tau)\, d\tau + c_d \Delta e_i(t)\right\}, 1\right\}. \tag{6}$$

It has been observed that this PID control strategy reduces numerical instabilities and improves convergence performance of the HCA algorithm.

### 4.2. Optimization problem

Previous work has shown that the HCA method is an effective topology synthesis technique, although not being a formal topology optimization method itself [10]. The basic premise of the HCA method is that bone remodels to obtain a state of stimulus equilibrium. This occurs when the stimulus error $e_i(t)$ in (4) goes to zero. This criterion applies to all the cells in the CA lattice. Tovar el al. showed that this criterion can be interpreted as the solution of a multiobjective structural optimization problem for minimizing both mass and strain energy written as

$$\min_{0 \leq x \leq 1} c(x) = f(U) + g(M), \tag{7}$$

where $f(U) = U/U_0$ is a function of the current strain energy $U$ and initial strain energy $U_0$, $g(M) = M/M_0$ is a function of the current mass $M$ and the initial mass $M_0$, and $x$ is the vector of relative densities for each cell [12]. Thus, the set of rules for conducting structural optimization with HCA are determined by deriving the Karush-Kuhn-Tucker (KKT) optimality conditions. The Lagrangian of the aforementioned optimization problem can be written as

$$L = f(U) + g(M) + (\lambda^1)^T (x - 1) - (\lambda^0)^T x, \tag{8}$$

where $\lambda^0$ and $\lambda^1$ are the Lagrange multiplier vectors associated with the inequality constraints. Subsequently, the KKT necessary conditions are given by

$$\frac{\partial L}{\partial x_i} = \frac{\partial f(U)}{\partial U}\frac{\partial U}{\partial x_i} + \frac{\partial g(M)}{\partial M}\frac{\partial M}{\partial x_i} + \lambda_i^1 - \lambda_i^0 = 0, \tag{9}$$

$$\lambda_i^1 \geq 0, \tag{10}$$

$$\lambda_i^0 \geq 0, \tag{11}$$

$$\lambda_i^1(x_i - 1) = 0, \tag{12}$$

and

$$\lambda_i^0 x_i = 0. \tag{13}$$

4.3. Optimality conditions

The KKT necessary conditions specify the criterion to be satisfied for both interior and saturated points. For an interior point, i.e., $0 < x_i < 1$, by definition the Lagrange multipliers are $\lambda_i^1 = \lambda_i^0 = 0$, satisfying (10)–(13). Therefore, the optimality conditions are satisfied if

$$\frac{\partial f(U)}{\partial U}\frac{\partial U}{\partial x_i} + \frac{\partial g(M)}{\partial M}\frac{\partial M}{\partial x_i} = 0. \tag{14}$$

For the case that $f(U) = \omega_1 U$ and $g(M) = \omega_2 M$, then (14) yields the optimality condition

$$S_i = S_i^* \equiv \frac{\omega_2}{\omega_1}\frac{\rho_{0i}}{p}, \tag{15}$$

where $\rho_{0i}$ is the density of a solid element [12].

For either case where the relative density $x_i$ is saturated, i.e., $x_i = 0$ or $x_i = 1$, different optimality conditions apply. For the case of $x_i = 0$, it follows from (12) that $\lambda_i^1 = 0$. Therefore, the conditions in (10), (12), and (13) are satisfied. The remaining optimality conditions from (9) and (11) can then be combined to yield,

$$\lambda_i^0 = \left.\frac{\partial f(U)}{\partial U}\frac{\partial U}{\partial x_i}\right|_{x_i=0} + \left.\frac{\partial g(M)}{\partial M}\frac{\partial M}{\partial x_i}\right|_{x_i=0} \geq 0. \tag{16}$$

If it is assumed that $f(U) = \omega_1 U$ and $g(M) = \omega_2 M$, it has been shown that (16) leads to the optimality condition,

$$\lambda_i^0 = \omega_2 m_{0i} \geq 0. \tag{17}$$

This condition implies that $0 = S_i \leq S_i^*$ if $x_i = 0$.

In the case that $x_i = 1$, it follows from (13) that $\lambda_i^0 = 0$. Therefore, the conditions in (11), (12), and (13) are satisfied. The remaining optimality conditions from (9) and (10) can be combined to yield,

$$\lambda_i^1 = -\left.\frac{\partial f(U)}{\partial U}\frac{\partial U}{\partial x_i}\right|_{x_i=1} - \left.\frac{\partial g(M)}{\partial M}\frac{\partial M}{\partial x_i}\right|_{x_i=1} \geq 0. \tag{18}$$

Again, utilizing the assumption that $f(U) = \omega_1 U$ and $g(M) = \omega_2 M$, it has been shown that (18) yields the optimality condition,

$$\lambda_i^1 = \omega_1 p v_{0i}\left.\frac{U_i}{x_i}\right|_{x_i=1} - \omega_2 m_{0i} \geq 0, \tag{19}$$

which can be written as

$$\left.\frac{U_i}{x_i}\right|_{x_i=1} \geq \frac{\omega_2}{\omega_1}\frac{\rho_{0i}}{p}. \tag{20}$$

This condition implies that $S_i|_{x_i=1} \geq S_i^*$ if $x_i = 1$.

4.4. Proof of convergence

In previous work, it has been observed that the convergence of the HCA methodology is affected by parameters of the algorithm. To utilize HCA as a generic topology synthesis tool, it is important to understand

the conditions under which HCA converges to an optimal design. A previous study proved that HCA is a fixed point algorithm,

$$x(t+1) = G(x(t)), \tag{21}$$

where $G(x(t))$ is the function representing the HCA update [16]. In mathematics, a fixed point $\bar{x}$ of a function $G(x)$ is a point that is mapped to itself by the function: $G(\bar{x}) = \bar{x}$ [24]. There are numerous theorems in different parts of mathematics that guarantee that these functions, if they satisfy certain conditions, have at least one fixed point. If the HCA iteration is converging to a fixed point $\bar{x}$, then it must be true that

$$\|x(t+1) - \bar{x}\| \to 0. \tag{22}$$

Using (21), the definition of a fixed point, and the Mean Value Theorem gives

$$\|x(t+1) - \bar{x}\| = \|G(x(t)) - G(\bar{x})\| = \|DG(\hat{x})(x(t) - \bar{x})\| \leq \|DG(\hat{x})\| \, \|(x(t)) - \bar{x})\| \tag{23}$$

for any vector norm $\|\cdot\|$ and for some $\hat{x}$ between $\bar{x}$ and $x(t)$. This holds for $0 < x_i(t) < 1$, and also at the boundary values if $x_i(t) = \bar{x}_i = 0$ or $x_i(t) = \bar{x}_i = 1$.

If the operator norm

$$\|DG(\hat{x})\| \leq L < 1 \tag{24}$$

for some constant $L$, vector norm $\|\cdot\|$, and every $\hat{x}$, then $G(x)$ has a unique fixed point $\bar{x}$ and the HCA iteration converges to $\bar{x}$ for any starting point $0 < x_i(0) < 1$ (this is the contraction mapping theorem). For each $\epsilon > 0$ there exists a vector norm $\|\cdot\|$ such that

$$\rho(DG(\bar{x})) \leq \|DG(\bar{x})\| < \rho(DG(\bar{x})) + \epsilon, \tag{25}$$

where

$$\rho(DG(\bar{x})) = \max_{1 \leq j \leq s} |\lambda_j| \quad (\lambda_1, \ldots, \lambda_s \text{ are the eigenvalues of } DG(\bar{x})) \tag{26}$$

is the spectral radius of the Jacobian matrix $DG(\bar{x})$, and (25) holds for all $x$ in a neighborhood of $\bar{x}$ [24]. Hence if

$$\rho(DG(\bar{x})) < 1, \tag{27}$$

then the HCA iteration converges to the fixed point $\bar{x}$ for any initial $x(0)$ sufficiently close to $\bar{x}$ . Note that if $DG(x)$ is symmetric, then $\|DG(x)\|_2 = \rho(DG(x))$, and so $\rho(DG(x)) < 1$ on $0 \leq x \leq 1$ would guarantee HCA converges for any $0 \leq x(0) \leq 1$ . For nonsymmetric $DG(x)$, the norm in (25) changes with $x$, so HCA convergence is guaranteed only in a neighborhood of $\bar{x}$.

### 4.5. Implementation

Recently, it has been questioned if the designs produced by HCA when utilizing neighborhood information satisfy the KKT optimality conditions. In fact, topologies synthesized using neighborhood information have been presented by Tovar et al. that do not satisfy the all of the optimality criterion [10, 12]. In these examples, an insufficient criterion was utilized to determine when a fixed point had been reached. For instance, the Mitchell truss examples presented by Tovar et al. utilized a HCA stopping criterion

$$|M(t+1) - M(t)| \leq \epsilon, \tag{28}$$

where $M(t)$ is the mass of the structure at a time $t$ and $\epsilon = 0.001 \cdot M_0$, for the initial structural mass $M_0$ [12]. This criterion is global in nature and it does not ensure that all of the optimality conditions are satisfied. For the cells that have saturated, their local changes in relative density will become zero and their respective optimality criterion will be satisfied. However, this stopping criterion does not yield any meaningful measure of the satisfaction of the optimality criterion for an interior point (i.e., $S_i(t) - S_i^* \not\to 0$). It is possible that the criterion of (28) is satisfied while large local changes in relative density $x_i$ are still occurring, as in [10, 12]. While the optimality conditions are not strictly satisfied, the number of interior points represents $< 2\%$ of the number of elements in the structures presented in Tovar et al. [10, 12].

For the purpose of mathematical rigor, an algorithm stopping criterion will be used that ensures that the optimality conditions for all cells are satisfied. From the definition of a fixed point iterative scheme in

(21), it would be reasonable to define a criterion that ensures that the local changes in relative density $x_i$ are sufficiently small, i.e.,

$$|x_i(t+1) - x_i(t)| \leq \epsilon. \tag{29}$$

This criterion is more meaningful in the sense that it is the same for every cell.

Considering an HCA update that only utilizes proportional control (i.e., $c_i = c_d = 0, c_p \neq 0$), the expression from (6) can be rewritten as,

$$x_i(t+1) = x_i(t) + c_p e_i(t), \tag{30}$$

for $0+\epsilon \leq x_i(t) \leq 1-\epsilon$. Rearranging (30) and substituting into (29) yields the satisfaction of the optimality criterion

$$|e_i(t)| = |S_i(t) - S_i^*| \leq \frac{\epsilon}{|c_p|}. \tag{31}$$

Thus, one must carefully consider the algorithm stopping criterion so as to be able to appropriately assess the optimality of the obtained $x(t)$. In this investigation, the stopping criterion was (29) with $\epsilon = 5 \cdot 10^{-4}$.

## 5. Neighboring reduction technique

Utilizing neighborhood information is a method of dampening the local changes in the relative density $x_i$. It will be shown that it is not always possible to achieve a mathematically optimal solution when using neighborhood information. This is because the neighborhood averaging is driving $\bar{S}_i(t) - S_i^* \to 0$, which does not imply $S_i(t) - S_i^* \to 0$. This due to the fact that the optimality condition was derived for the case when $\hat{N} = 0$. In this study, it is desired to utilize neighborhood information to avoid computational instability and checkerboarding. Previous studies have utilized a constant neighborhood throughout the entire synthesis process. These conventional fixed neighborhood schemes will be compared with sequential neighboring and adaptive neighboring techniques.

### 5.1. Sequential neighboring

For the sequential neighboring strategy, an initial neighborhood size $\hat{N}^0$ and final neighborhood size $\hat{N}^\infty$ will be selected. An initial design will be synthesized utilizing $\hat{N}^0$, until the algorithm stopping criterion is achieved. The initial design will then be used as the starting point for topology synthesis when utilizing $\hat{N}^\infty$, producing the final design. The premise behind the sequential neighboring scheme is that although the structures generated with fixed neighborhoods may not satisfy the optimality criterion, it is possible that they provide a suitable starting point for an improved design.

### 5.2. Adaptive neighboring

For the adaptive neighboring strategy, the influence of each neighbor $w_k$ is incorporated in the effective stimulus calculation. Recall that the effective stimulus in (2) weights the stimulus of a cell and its neighbors equally. Rewriting this equation to include the influence of each neighbor $w_k$ yields

$$\bar{S}_i(t) = \frac{S_i(t) + \sum_{k \in N(i)} w_k(t) S_k(t)}{1 + \sum_{k \in N(i)} w_k(t)}. \tag{32}$$

One strategy for weighting each neighbor is to calculate the influence of a neighboring cell based on that cell's closeness to the algorithm stopping criterion in (29). This can be represented as a piecewise-linear function with weights ranging between 0 and 1 for changes in the local relative density of the neighboring elements, i.e., $|x_k(t) - x_k(t-1)|$ (Fig. 1). Thus, the neighbor weights can be expressed as

$$w_k(t) = \min\left\{\max\left\{0, \frac{|x_k(t) - x_k(t-1)| - \Delta^0}{\Delta^1 - \Delta^0}\right\}, 1\right\}, \tag{33}$$

where $\Delta^1$ is the minimum change in relative density of the $k$th neighbor for which its weight is 1, and $\Delta^0$ is the maximum change in relative density of the $k$th neighbor for which its weight is 0. Note that $\Delta^0 > \epsilon$ to ensure that the weights of all neighbors are zero when the stopping criterion is met. Therefore, the effective size of the neighborhood will be $\hat{N} = 0$ when the topology synthesis is complete.

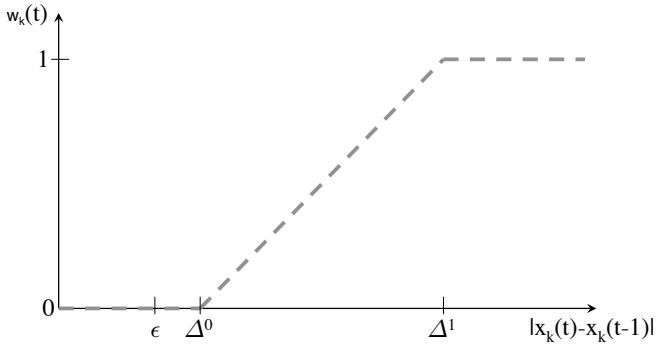


Figure 1: Piecewise-linear representation for neighborhood weights $w_k$.

The reasoning behind this neighbor weighting scheme is that the optimality conditions for interior and saturated points are different. It is reasonable that any number of cells may have a neighbor which is converging to an optimality condition other than that of the current cell. For example, this situation would arise when a cell saturated at full density is in the neighborhood of a cell with intermediate density. If it is not possible for the cell of intermediate density to become saturated, then the influence of the fully dense neighbor would not be consistent with achieving the optimality condition for an interior point. Thus, allowing the influence of neighboring cells that are undergoing sufficiently small changes in relative density to decrease to zero will eliminate the adverse influence of neighbors that are converging to different optimality conditions.

## 6. Comparative studies

The effect of incorporating neighborhood information was assessed by studying an empty neighborhood, fixed neighborhood, sequential neighboring, and the aforementioned adaptive neighboring technique. These techniques were applied to a simply supported structure modeled with $50 \times 25$ cells (Fig. 2), as done in Tovar et al. [12]. For this example, a one to one mapping is used between the cells of the CA lattice and the FE model. Quadrilateral bilinear finite elements are used. The node at the bottom left corner is constrained in both coordinate directions to have zero displacement so that the node is fixed, while the node in the bottom right corner is constrained only in the vertical direction to resemble a rolling support. A downward force of 100 N is applied to the node at the midspan of the bottom edge. The dimensions of the structure are 25 mm in width by 50 mm in height. As mentioned before, the HCA algorithm operates on the relative density of each cell, therefore, the density is interpolated between zero and one, using a power law relationship (3) with exponent $p = 3$. The initial structure was assumed to be fully dense (i.e., $x_i = 1$ for all $i$). The Young's modulus was set at $E = 20$ GPa and the Poisson's ratio to $\nu = 0.3$. The equilibrium stimulus was set at $S_i^* = 1.8084 \cdot 10^{-9}$ Pa for all $i$, i.e., each cell in the lattice is seeking the same target stimulus. For this equilibrium stimulus, it can be shown using (15) that the corresponding objective function weights in (7) are $\omega_1 = 0.25$ and $\omega_2 = 0.75$. The CA implementation used for the following numerical experiments is given in (6) for $c_p = 0.2, c_i = 0$, and $c_d = 0$.

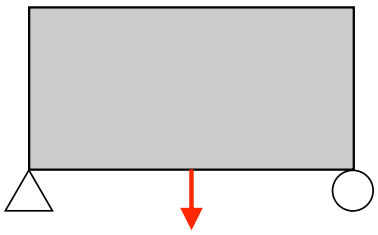

Figure 2: Simply supported $50 \times 25$ beam structure.

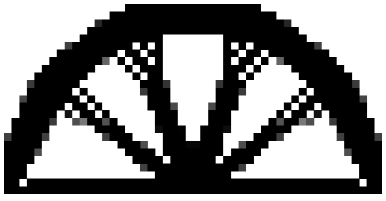

Figure 3: Structure generated with $\hat{N} = 0$ in 81 iterations. This structure is optimal and has a final objective function value of $c = 0.73646$.

### 6.1. Empty neighborhood

In this first example, a design was synthesized utilizing an empty neighborhood, i.e., $\hat{N} = 0$ (Fig. 3). One

can see that this design contains checkerboarding, which makes it undesirable to a designer. However, in terms of the objective this design has met the algorithm stopping criterion in (29) and satisfies the optimality criterion within the specified tolerance in (31). The objective function value for this structure is $c = 0.73646$ and was obtained in 81 iterations.

6.2. Nonzero neighborhood

To compare the empty neighborhood result with those of typical 2D CA neighborhoods, structures were generated while using von Neumann ($\hat{N} = 4$) and Moore ($\hat{N} = 8$) neighborhoods. In both cases significantly more iterations were required to meet the local stopping criterion in (29), as compared to the empty neighborhood case. For $\hat{N} = 4$, the structure was synthesized in 237 iterations with a function value of $c = 0.74488$ (Fig. 4). For $\hat{N} = 8$, the structure was synthesized in 753 iterations with a function value of $c = 0.74312$ (Fig. 5). The objective function value in both cases is larger than that of the empty neighborhood result.

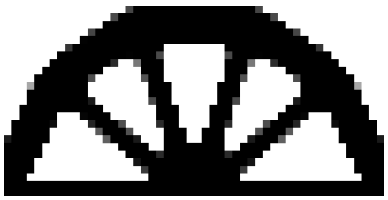

Figure 4: Structure generated with $\hat{N} = 4$ in 237 iterations. This structure is not optimal and has a final objective function value of $c = 0.74488$.

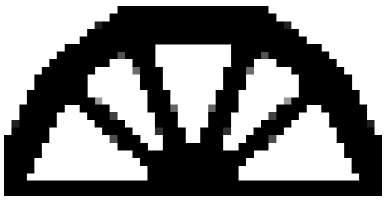

Figure 5: Structure generated with $\hat{N} = 8$ in 753 iterations. This structure is not optimal and has a final objective function value of $c = 0.74312$.

Although the generated structures do not contain any checkerboarding, these structures do not satisfy the optimality criterion and are not local minima. This is due to the fact that $\bar{S}_i - S_i^* \to 0$, which does not imply that the optimality condition $S_i - S_i^* \to 0$. However, these solutions are indeed fixed points of the HCA iteration function given in (6), for their respective neighborhood sizes.

6.3. Sequential neighboring

The previous structures generated with nonzero neighborhoods are not optimal, however they provide a suitable starting point for an improved design. For this reason the sequential neighborhood strategy was employed where the $\hat{N}^0 = 4$ and $\hat{N}^\infty = 0$, and $\hat{N}^0 = 8$ and $\hat{N}^\infty = 0$. This will allow each element in these designs to meet both the stopping criterion and the optimality criterion within the specified tolerance, yet retain the benefits of utilizing neighborhood information. For $\hat{N}^0 = 4$ and $\hat{N}^\infty = 0$, the structure was synthesized in 299 iterations with a function value of $c = 0.74008$ (Fig. 6). For $\hat{N}^0 = 8$ and $\hat{N}^\infty = 0$, the structure was synthesized in 810 iterations with a function value of $c = 0.73880$ (Fig. 7). The objective function value in both cases is larger than that of the empty neighborhood result.

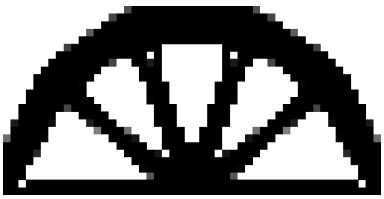

Figure 6: Structure generated with $\hat{N}^0 = 4$ and $\hat{N}^\infty = 0$ in 299 iterations. This structure is optimal and has a final objective function value of $c = 0.74008$.

Figure 7: Structure generated with $\hat{N}^0 = 8$ and $\hat{N}^\infty = 0$ in 810 iterations. This structure is optimal and has a final objective function value of $c = 0.73880$.

Again, these structures contain little to no checkerboarding. The objective function values decreased as compared to the nonzero neighborhood results, but are still slightly larger than that for the empty neighborhood used for the entire synthesis process. For completeness, the opposite simulations were conducted, $\hat{N}^0 = 0$ and $\hat{N}^\infty = 4$, and $\hat{N}^0 = 0$ and $\hat{N}^\infty = 8$. Both of these cases yielded the same result as the empty neighborhood case in the same number of iterations, which was expected. This is due to the fact that

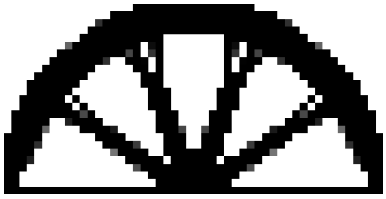

(a) $\Delta^1 = 0.20, c = 0.73251$, 77 iterations

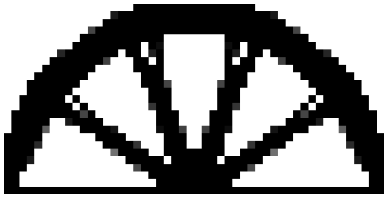

(b) $\Delta^1 = 0.15, c = 0.73222$, 137 iterations

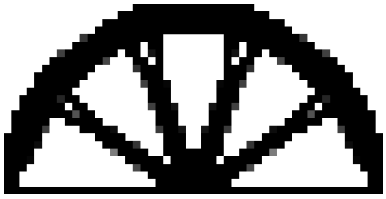

(c) $\Delta^1 = 0.10, c = 0.73327$, 100 iterations

(d) $\Delta^1 = 0.05, c = 0.73265$, 81 iterations

Figure 8: Adaptive neighboring strategy with $\hat{N} = 4$. Each structure is optimal and represents a local minimum.

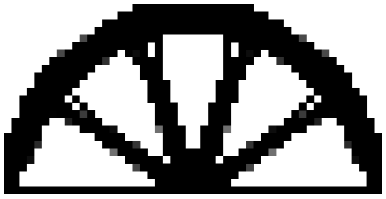

(a) $\Delta^1 = 0.20, c = 0.73216$, 88 iterations

(b) $\Delta^1 = 0.15, c = 0.73178$, 83 iterations

(c) $\Delta^1 = 0.10, c = 0.73244$, 130 iterations

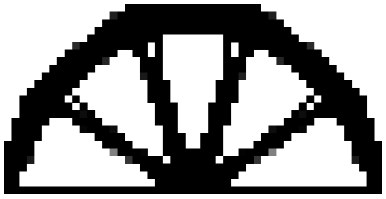

(d) $\Delta^1 = 0.05, c = 0.73120$, 4338 iterations

Figure 9: Adaptive neighboring strategy with $\hat{N} = 8$. Each structure is optimal and represents a local minimum.

each cell has already met the specified stopping criterion tolerance, therefore, the average change over the neighborhood will be within the tolerance as well.

6.4. Adaptive neighboring

The adaptive neighboring strategy incorporates a new method for weighting the influence $w_k$ of neighbors. For this study, fix $\Delta^0 = 0.001 > \epsilon = 5 \cdot 10^{-4}$. The selection of $\Delta^1$ will determine the steepness of the transition between $w_k = 1$ and $w_k = 0$. Topologies were synthesized for $\Delta^1 = 0.20, 0.15, 0.10, 0.05$, selected based on the value of $c_p = 0.20$. Since the error is normalized in (4), a large change in relative density in (6) would be on the order of $c_p$. To compare this strategy with the previous examples the same 2D CA neighborhoods were utilized, von Neumann ($\hat{N} = 4$) and Moore ($\hat{N} = 8$). The results for $\hat{N} = 4$ and $\hat{N} = 8$ are displayed in Figures 8 and 9, respectively.

It is interesting to note that all of the structures synthesized for both $\hat{N} = 4$ and $\hat{N} = 8$ are improved designs as compared to the empty neighborhood result. The topologies with the best objective function value were obtained with $\Delta^1 = 0.15$ for $\hat{N} = 4$ and $\Delta^1 = 0.05$ and for $\hat{N} = 8$. From these results, it is not apparent that the reduction in $\Delta^1$ is related to either a decrease in objective function value or the number of iterations required to carry out the design synthesis. However, it was found that if $\Delta^1$ is too close to $\Delta^0$

oscillations are induced in the synthesis process, delaying the arrival at the final design. This is apparent from Fig. 9(d), for which the design synthesis required over 4000 iterations.

## 7. Final comments

This study shows that it is possible to retain the benefits from utilizing neighborhood information and obtain an optimal solution with HCA. Several different neighborhood schemes were analyzed, an empty neighborhood, fixed neighborhood, sequential neighboring, and adaptive neighboring. Optimal designs were synthesized in each case, with the exception of fixed neighborhoods. Compared to the empty neighborhood algorithm, the sequential neighboring technique produced optimal designs with little to no checkerboarding, but at a significant increase in iterations; the adaptive neighboring scheme produced optimal designs with less checkerboarding and an improved objective function value; the adaptive method typically achieved the algorithm stopping criterion in a similar number of iterations. Therefore, it seems as though the adaptive neighboring rule is a good compromise between achieving the benefits of neighborhood smoothing, mathematical optimality, and algorithm speed.

Several important facts about neighborhoods are revealed by this study. (1) A global stopping criterion, such as that on the change in mass in (28), gives no meaningful measure of the satisfaction of the optimality conditions for an interior point. It is necessary to use a local stopping criterion due to the existence of interior points to ensure that the optimality conditions are explicitly satisfied. (2) Increasing the neighborhood size does not speed up the synthesis process. While these designs typically have less checkerboarding than the empty neighborhood design, the results of this study show that the use of a neighborhood can significantly slow down convergence to a local stopping criterion. (3) The use of neighborhood averaging in general leads to conflicting objectives when an interior point contains neighbors that are saturated points, a situation where the cell and its neighbors are approaching different optimality conditions. Neighborhood averaging will not allow the interior point to achieve its optimality criterion as illustrated by the fixed neighborhood results here.

## 8. Acknowledgements

This research effort was supported in part by the following grants and contracts: a grant from Honda Research and Development Americas, Inc., and the National Science Foundation grants DMI-0422719, DMI-0355391, CMMI 08-00290, and CMII 07-00730.

## 9. References

[**1**] G.I.N. Rozvany. A critical review of established methods of structural topology optimization. *Struct. Multidisc. Optim.*, 37(3):217–237, 2009.

[**2**] M.P. Bendsøe. Optimal shape design as a material distribution problem. *Comput. Methods Appl. Mech. Eng.*, 1:193–202, 1989.

[**3**] Y. M. Xie and G.P. Stevens. *Evolutionary Structural Optimization*. Springer-Verlag, London, 1997.

[**4**] K. Svanberg. The method of moving asymptotes: A new method for structural optimization. *Int. J. Numer. Meth. Engrg.*, 24:359–373, 1987.

[**5**] M.P. Bendsøe and N. Kikuchi. Generating optimal topologies in optimal design using a homogenization method. *Comput. Methods Appl. Mech. Eng.*, 71:197–224, 1988.

[**6**] N. Inou, T. Uesugi, A. Iwasaki, and S. Ujihashi. Self-organization of mechanical structure by cellular automata. *Key Eng. Mat.*, 145/149(2):1115–1120, 1998.

[**7**] E. Kita and T. Toyoda. Structural design using cellular automata. *Struct. Multidisc. Optim.*, 19:64–73, 2000.

[**8**] P. Hajela and B. Kim. On the use if energy minimization for ca based analysis in elasticity. *Struct. Multidisc. Optim.*, 23:24–33, 2001.

[**9**] A. Tovar. Optimización topológica con la técnica de los autómatas celulares híbridos. *Revista Internacional de Métodos Numéricos para el Cálculo y Diseño en Ingeniería*, 21(4):365–383, 2005.

[**10**] A. Tovar, N.M. Patel, G.L. Niebur, M. Sen, and J.E. Renaud. Topology optimization using a hybrid cellular automaton method with local control rules. *ASME J. Mech. Des.*, 128(6):1205–1216, 2006.

[**11**] M.M. Abdalla, S. Setoodeh, and Z. Gürdal. Cellular automata paradigm for topology optimisation. In M.P. Bendsøe, N. Olhoff, and O. Sigmund, editors, *IUTAM Symposium on Topological Design Optimization of Structures, Machines and Materials*, pages 169–180. Springer, 2006.

[**12**] A. Tovar, N. Patel, A. K. Kaushik, and J.E. Renaud. Optimality conditions of the hybrid cellular automata for structural optimization. *AIAA J.*, 45(3):673–683, 2007.

[**13**] A. Tovar, W.I. Quevedo, N.M. Patel, and J.E. Renaud. Topology optimization with stress and displacement constraints using the hybrid cellular automaton method. In *Proceedings of the 3rd European Conference on Computational Mechanics*, Lisbon, Portugal, June 5-8 2006.

[**14**] N.M. Patel, A. Tovar, and J.E. Renaud. Compliant mechanism design using the hybrid cellular automaton method. In *1st AIAA Multidisciplinary Design Optimization Specialist Conference*, Austin, Texas, April 18-21 2005.

[**15**] N.M. Patel, B.S. Kang, J.E. Renaud, and A. Tovar. Crashworthiness design using topology optimization. *ASME J. Mech. Des.*, 131(6), 2009.

[**16**] C.L. Penninger, L.T. Watson, A. Tovar, and J.E. Renaud. Convergence analysis of hybrid cellular automata for topology optimization. *Struct. Multidisc. Optim.*, 2009.

[**17**] A. Tovar. *Bone Remodeling as a Hybrid Cellular Automaton Optimization Process*. PhD thesis, University of Notre Dame, 2004.

[**18**] A. Diaz and O. Sigmund. Checkerboard patterns in layout optimization. *Struct. Optim.*, 10(1):40–45, 1995.

[**17**] A. Diaz and O. Sigmund. Checkerboard patterns in layout optimization. *Struct. Optim.*, 10(1):40–45, 1995.

[**18**] O. Sigmund and J. Petersson. Numerical instabilities in topology optimization: A survey on procedures dealing with checkerboards, mesh-dependencies and local minima. *Struct. Multidisc. Optim.*, 16(1):68–75, 1998.

[**19**] J.D. Currey. The effect of porosity and mineral-content on the Young's modulus of elasticity of compact-bone. *J. Biomech.*, 21:131–139, 1998.

[**20**] D.P. Fyhrie and D.R. Carter. A unifying principle relating stress to trabecular bone morphology. *J. Orthop. Res.*, 4:304–317, 1986.

[**21**] R. Huiskes, H. Weinans, H.J. Grootenboer, M. Dalstra, B. Fudala, and T.J. Slooff. Adaptive bone-remodeling theory applied to prosthetic-design analysis. *J. Biomech.*, 20:1135-1150, 1987.

[**22**] R. Huiskes, R. Ruimerman, G.H. van Lenthe, and J.D. Janssen. Effects of mechanical forces on maintenance and adaptation of form in trabecular bone. *Nat.*, 405:704-706, 2000.

[**23**] R. Ruimerman, P. Hilbers, B. van Rietbergen, and R. Huiskes. A theoretical framework for strain-related trabecular bone maintenance and adaptation. *J. Biomech.*, 38:931-941, 2005.

[**24**] E. Isaacson and H.B. Keller. *Analysis of Numerical Methods*. Wiley, New York, 1966.